Interference Mitigation Techniques in 60 GHz Wireless Networks

Minyoung Park, Praveen Gopalakrishnan, and Richard Roberts, Intel Corp.

ABSTRACT

In recent years, the unlicensed 60 GHz band has motivated the computer, wireless communications, and consumer electronics industries to develop wireless personal area network and wireless local area network standards that support wireless applications with multigigabit data rates. One of the technical challenges is managing interference between networks in a dense environment. In this article we first show the problem of interference in a dense environment and evaluate and compare PHY and MAC layer interference mitigation techniques in terms of performance and the level of co-ordination required among interfering networks.

INTRODUCTION

In the 60 GHz frequency spectrum band (57~64 GHz in the United States, Canada, and Korea, 59~66 GHz in Japan, 57~66 GHz in Europe), 7~9 GHz wide unlicensed spectrum is available globally [1]. Comparing this to the 2.4 GHz industrial, scientific, and medical (ISM) band and 5 GHz unlicensed national information infrastructure (UNII) bands where Wi-Fi is used, the 60 GHz band has more than 10 times wider spectrum.

In recent years, the abundant unlicensed spectrum in the 60 GHz band and advances in complementary metal oxide semiconductor (CMOS) technology [2] have motivated computer, wireless communications, and consumer electronics industries as well as the research community to form a number of standardization bodies (ECMA TC48 [3], IEEE 802.15.3c [4], WirelessHD [5], IEEE 802.11ad [6]) to develop standards to utilize the resources available in the 60 GHz band for wireless personal area network (WPAN) and wireless local area network (WLAN) applications.

In most standards work, a common usage model is transferring a high-quality video stream over a wireless channel in home and office environments. The usage cases are wireless high-definition video streaming from a video source (e.g., set-top box) to the display in a living room, and the wireless connection between a laptop and a monitor in an office cubicle. To overcome much higher free space propagation loss in a 60 GHz channel due to the short wavelength [7], typically antenna arrays with multiple antenna elements are used for beamforming, which coherently adds up the signals sent and received from the multiple antenna elements [8]. To support very high data rates (e.g., 3 Gb/s for 1080-pixel high definition video quality) and stringent latency requirements for high-quality video streaming, ECMA TC48, IEEE 802.15.3c, and WirelessHD support four non-overlapping channels, each with 2.16 GHz bandwidth, and the medium typically accessed in time-division multiple access (TDMA) fashion for isochronous traffic such as uncompressed or compressed video.

There are, however, only three non-overlapping channels available in most countries due to 7 GHz wide spectrum (the only exception is Europe with 9 GHz). Although it is easier to guarantee quality of service (QoS) for an application by reserving time periods for data transmission and reception, as the environment gets denser with more and more wireless networks neighboring each other, it becomes harder to manage interference between the neighboring networks. An office cubicle environment is a good example that shows such a scenario where small cubicles are neighboring two or three other users, each cubicle forming its own WPAN transmitting a video stream from the laptop to the display independently. This motivates our study of physical layer (PHY) and medium access control (MAC) layer interference mitigation (IM) techniques for 60 GHz wireless networks. In the following sections a number of IM techniques are compared in terms of performance and the complexity of coordination among the interfering networks.

INTERFERENCE PROBLEM IN A DENSE OFFICE ENVIRONMENT

Although beamforming inherently mitigates interference due to narrow beam width, the interference problem can easily be found in a dense office environment as shown in Fig. 1. We conducted simulations to evaluate the impact of co-channel interference from neighboring cubicles.

SIMULATION SETUP

We assume four office cubicles as shown in Fig. 1. The dimensions of the cubicle are 3 m × 2 m × 3 m (width × length × height). Each cubicle

0163-6804/09/$25.00 © 2009 IEEE

has one notebook (NB) and one monitor, and the notebook transmits a video stream to the monitor. The arrangement of the devices is to show a possible interference scenario that may degrade application performance. Since there are only three non-overlapping channels available in most countries, two networks will end up using the same frequency channel. Three cases are examined: interference between Link1 and Link2, Link1 and Link3, and Link1 and Link4.

A square array antenna with 16 patch antenna elements is equipped on each device. The array antennas are placed on the devices perpendicular to the page and the array antennas are oriented with the angles shown in Fig. 1. The radiation pattern of the antenna element is shown in Fig. 2. The antenna element has a cardioid shaped radiation pattern, which has unequal gain in different directions (i.e., elevation and azimuth angles). The 3 dB down beamwidth of the antenna element is approximately 90°, and the back lobe of the antenna pattern has 15 dB lower gain than the peak of the front lobe. The monitors are placed at the fixed locations shown in the figure, and the notebooks are randomly placed within the gray region (3/4 m × 2 m area). The total transmit power of the notebook is set to 10 dBm, and both the transmitter and receiver form beams in a traditional beamforming fashion toward each other as described in [8], but only controlling the phase of each antenna in π/8-step resolution to reduce the complexity of the devices. Path loss between a transmitter and a receiver is modeled based on the partition-based path loss model [9, 10]. We assume no reflectors within a cubicle and no walls between the neighboring cubicles.

Impact of Interference

Figure 3a shows the complementary cumulative distribution function (CDF) of signal-to-interference-plus-noise ratio (SINR) measured at the receivers of Link2, Link3, and Link4. If there is no interfering neighbor (rightmost dotted curve in Fig. 3a), the SINR of the link is higher than 28 dB, which is sufficient to support the highest data rate. However, if there is a neighboring network operating in the same channel, the SINR values of the receivers (solid curves) are degraded by approximately 18 dB and drop below 12 dB at the 90 percentile point. Depending on the PHY, this may be short of supporting the required data rates for the wireless display application. For IEEE 802.15.3c [4], the required sensitivity of high-rate PHY (HRP) mode index 0, which supports 0.952 Gb/s, is less than –50 dBm. Since the bandwidth of 802.15.3c is 1.76 GHz and assuming a noise figure of 7 dB and implementation loss of 5 dB, the required signal-to-noise ratio (SNR) is approximately 20 dB. In order to overcome the interference problem in a dense networking environment, we have investigated IM schemes in both the PHY and MAC layer.

PHY Interference Mitigation

Although an array antenna with many antenna elements is mainly used for beamforming to compensate for high free space propagation loss in the 60 GHz band, it can also be used for null-forming to mitigate interference. In this section a beam space nulling scheme and the simulation results are presented.

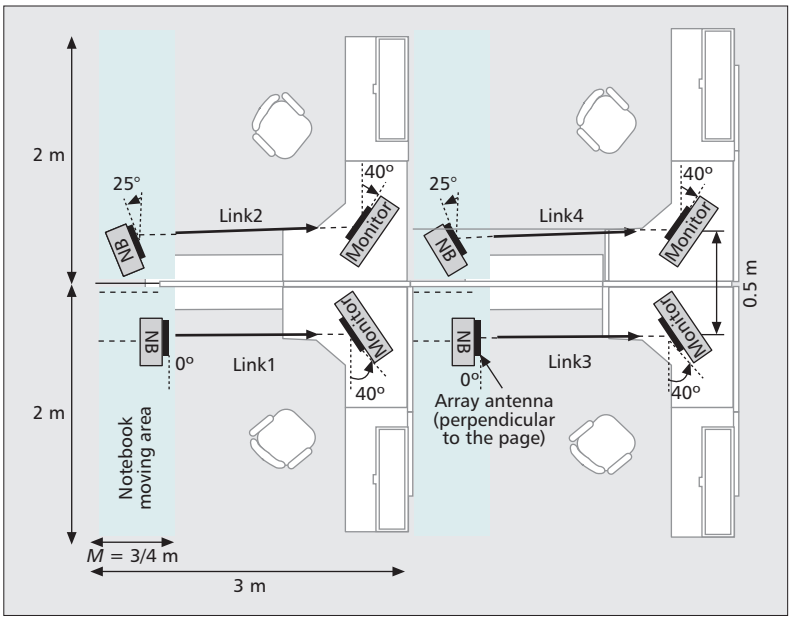

Figure 1. *Illustration of a dense office environment (NB = notebook). Two links are using the same frequency channel.*

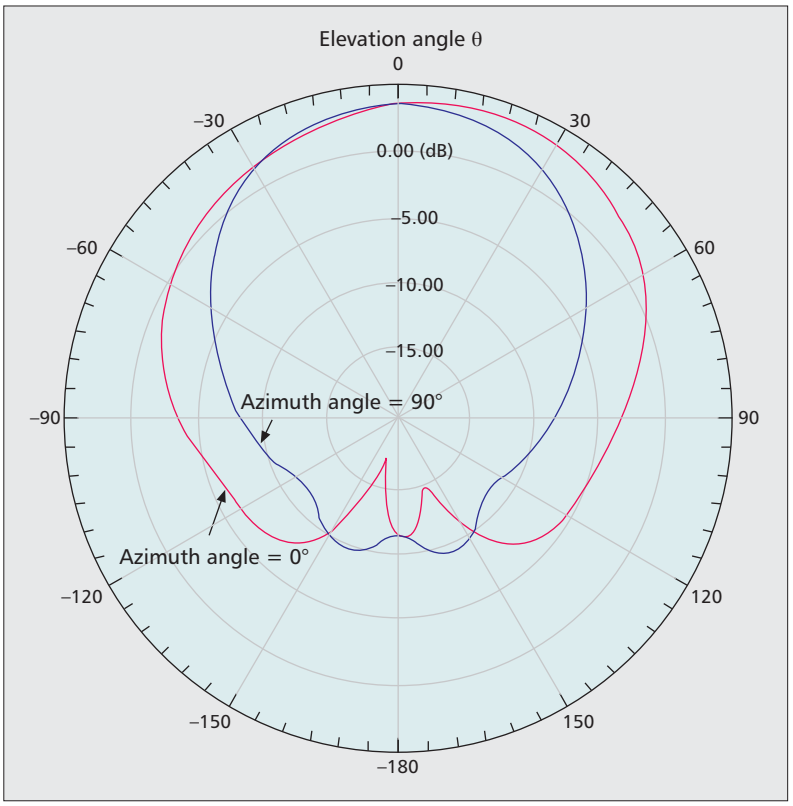

Figure 2. *Radiation patterns of the antenna element.*

Null-Forming in 60 GHz Band

Due to the desire to minimize complexity, it is anticipated that consumer 60 GHz beamforming implementations will operate in beam space [8] as shown in Fig. 4b. Using the receiver as an exam-

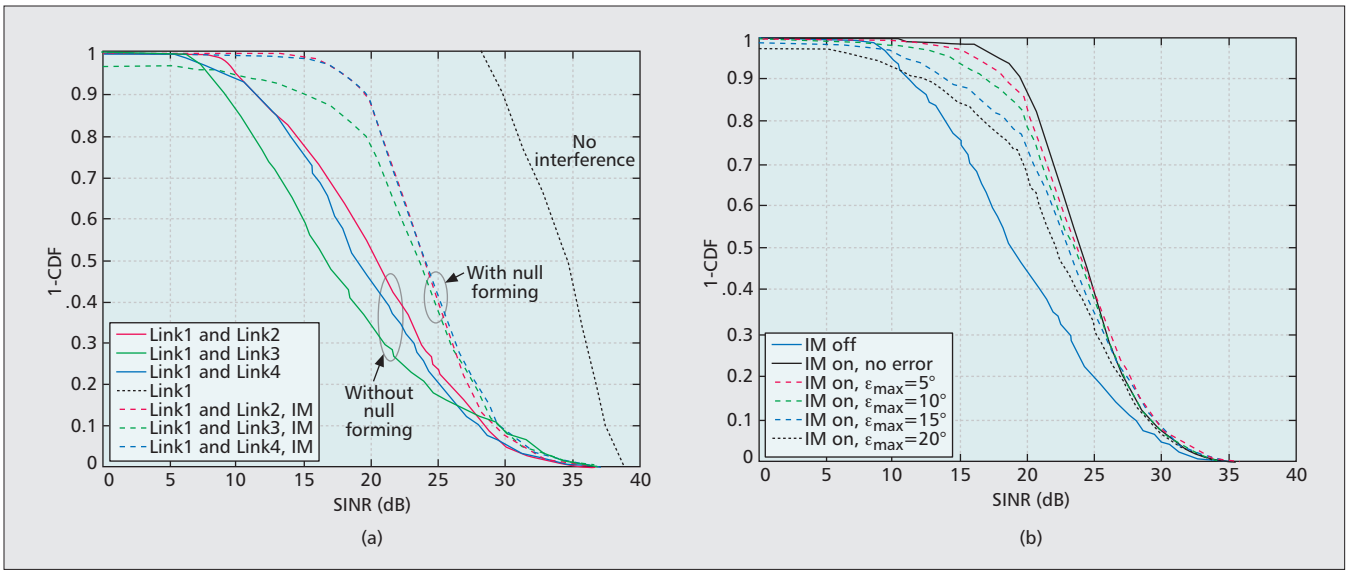

Figure 3. *Null-forming gain measurements: a) complementary CDF of SINR measured at the receivers with and without null-forming-based interference mitigation (IM) scheme; b) complementary CDF of SINR measured at the receiver of Link2 with and without estimation error in null-forming.*

ple, this means that coherent combining occurs in the analog domain prior to the sole analog-to-digital converter; hence, unlike multiple-input multiple-output (MIMO) — which operates in element space [8] as shown in Fig. 4a — beam space implementations do not have access to information present at the weights. This fact somewhat restricts the signal processing that can be used, but there is an abundance of research literature discussing beam space null-forming related to submarine acoustic tracking systems.

Figures 4b and 5 illustrate the basic idea of a beam space nulling scheme using a square antenna array with 36 antenna elements (6×6 configuration) operating in the azimuth plane. An interferer is located at a relative angle of 60°, while the signal of interest (SOI) is located at 50° as shown in Fig. 5a. It is desired that we only provide sufficient nulling of the interferer to obtain a desired signal-to-interference ratio (SIR). The basic procedure is to first determine the weight vector that points the beam at the interferer (i.e., a priori scan for interference) and then continue the scanning process until the SOI appears on the air, at which time the weight vector for the SOI is recorded. One simple way to scan for interference and the SOI is to try predefined beam patterns that point in different directions covering the whole space. As the number of beam patterns increases, the accuracy of finding the weight vectors for interference and the SOI increases, but at the same time the overhead of scanning also increases. The conjugate of the respective weight vectors is called the steering vector (since it respectively steers the beam). To illustrate, let $\underline{\mathbf{s}}_0$ and $\underline{\mathbf{s}}_i$ represent the SOI steering vector and steering vector for the ith interferer, respectively, as shown in Fig. 4b. In addition to storing the steering vectors, the related signal strength is stored so that the SIR can be estimated. The related signal processing is similar to the null-steering beamformer described in [8] and is straightforward inasmuch as we desire to find the weight vector $\underline{\mathbf{w}}$ that detects the SOI while providing additional nulling on the interference to achieve a desired SIR. It is better to use just enough interference nulling to achieve a desired SIR instead of forcing the interference to zero because this results in less distortion of the beam pattern in the direction of the SOI.

A typical beam pattern result is shown in Fig. 5b, where we have placed a 20 dB SIR null on the interferer at 60°, while substantially pointing the beam towards the SOI. In reality, we can see that while the interferer has been nulled, the beam has also rotated slightly clockwise attenuating the SOI by several dB. The cause of the main lobe attenuation toward the SOI is that the steering vectors are originally not orthogonal, along with the use of the pseudo inverse for inverting the rectangular matrix consisting of the steering vectors.

Simulation

To evaluate the null-forming gain, simulations are carried out using MATLAB. The office environment shown in Fig. 1 is used for the simulations. Only the receiver side forms a null toward the interference source. We first assume that there is no error in estimating the direction of the interference source. Later, we also show how an error in estimating the direction of the interference source affects the null-forming performance. Null-forming is performed only when the SIR measured at the receiver is lower than 20 dB, and interference is suppressed no more than 40 dB compared to the received signal power. Other settings are the same as the simulation settings used in the previous section. Note that only the phase of each antenna is controlled in $\pi/8$-step resolution.

Null-Forming Gain

The dashed curves shown in Fig. 3a show the complementary cumulative distributed function (CDF) of SINR measured at the receiver of each link using the null-forming-based IM. Compared to the cases where the receiver does not

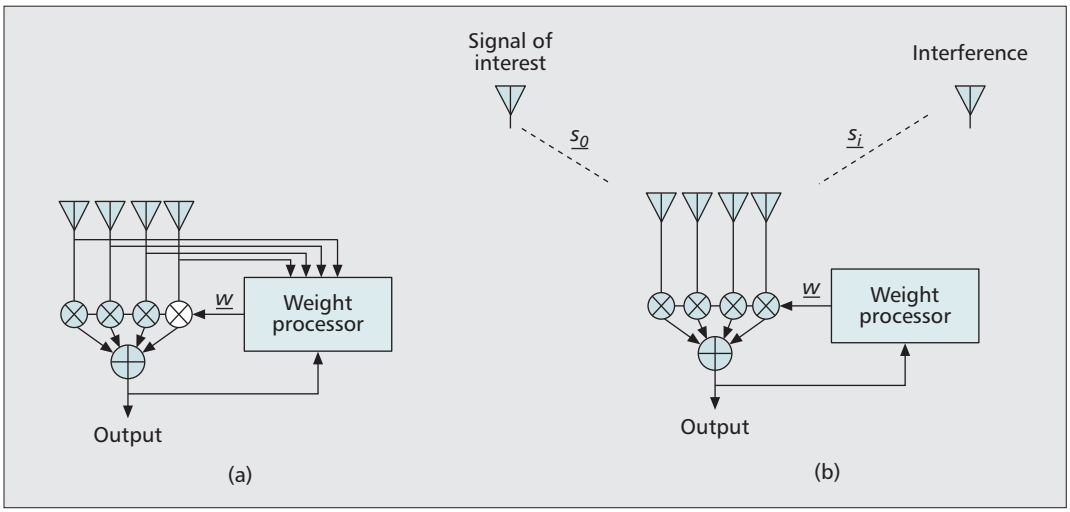

Figure 4. *Illustration of: a) element space processing; b) beam space nulling based on beam space processing. The objective of beam space nulling is to steer nulls toward the interference while maximizing the SOI SNR.*

For the cases of Link1-Link2 and Link1-Link4, the SINR of the link is maintained above 20 dB for approximately 90 percent, which provides very stable and high link quality to support sufficiently high data rate for wireless display applications.

have any IM scheme (the solid curves), the results show that the null-forming scheme significantly improves the link quality. For all three cases, the probability of maintaining the SINR above 20 dB is improved by at least 35 percent, which means that the links became more robust with the null-forming technique. In the case of Link1–Link3, the probability increases to 45 percent. For the cases of Link1–Link2 and Link1–Link4, the SINR of the link is maintained above 20 dB for approximately 90 percent of the transmission, which provides very stable and high link quality to support sufficiently high data rates for wireless display applications such as those described in the previous section.

Effect of Estimation Error on Null-Forming

To understand the impact of the estimation error on the performance of the null-forming, the estimation error ε is added to both elevation and azimuth angles of the direction of the interference source. The estimation error ε is modeled as a uniformly distributed random variable ranging between 0 and ε_{max}. Assuming Link1 and Link2 are operating in the same channel, the SINR at the receiver of Link2 is measured by varying ε_{max} from 0° (no error) to 20°. Figure 3b shows the complementary CDF of the SINR. The simulation results show that although the null-forming performance is degraded as the estimation error increases, the null-forming based IM scheme still provides significant gain. For example, for ε_{max} = 20°, the probability that Link2's SINR will be greater than 20 dB is improved by 25 percent compared to the case where the IM technique is not used (solid blue curve).

MAC Layer Interference Mitigation

There are various ways to mitigate interference among interfering WPANs at the MAC layer. The basic assumption we make is that the medium access scheme within each WPAN is TDMA for isochronous traffic applications such as video. This assumes that each WPAN has a network controller, responsible for scheduling the time slots based on inputs from the WPAN devices in the network. In such networks, time scheduling is the predominant mechanism to achieve IM. Various such mechanisms are possible by different types of scheduling, and their objective is to schedule interfering links in a non-overlapping fashion.

MAC Layer Interference Mitigation Techniques

We identify different techniques based on the level of coordination required among interfering WPANs. In general, the schemes listed below are listed in increasing order of co-ordination required among WPANs. It is expected that probability of success at IM will also increase with more coordination.

Simple TDMA — This is the baseline case where there is no coordination within or among WPANs and no information available regarding interference. In this situation it is very likely that no time scheduling technique is used, since there is no information regarding the presence or details of interference. This can be considered as the baseline case to understand performance degradation caused by interference, and performance improvement when we employ IM schemes.

Schedule Randomization — Here, the assumption is that limited coordination is available within each WPAN to indicate if there is interference. An example could be that the stations involving links that are interfered with, as observed by packet errors or delays, report back to the controller. Thus, the controller is made aware of the interference. However, the controller has no information on the times, severity, or source of interference. In the absence of detailed information about interference, the

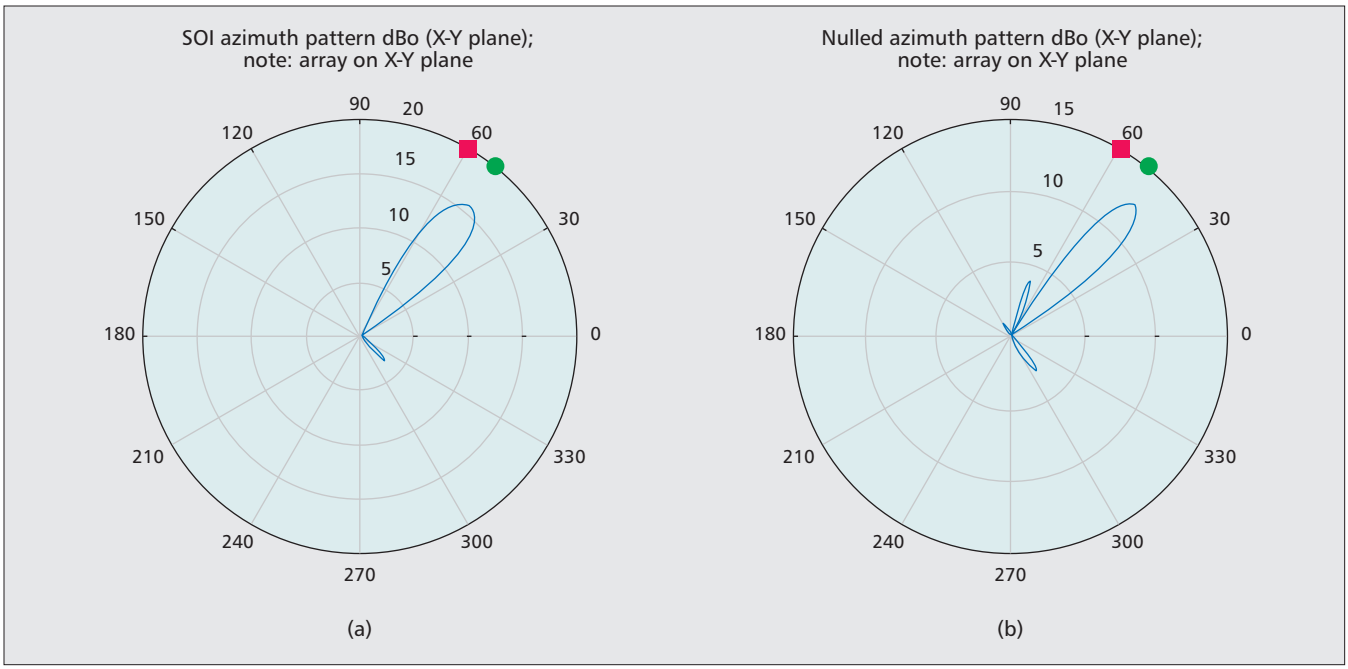

Figure 5. *An example of beam space nulling with a 6 × 6 isotropic square antenna array: a) interference at azimuth angle of 60° and the SOI at the azimuth angle of 50°; b) 20 dB constant SIR nulled beam.*

technique we considered is to change the existing schedule and randomly generate an alternate schedule in every new period of time.

Measure and Reschedule — This technique represents the case where there is coordination within each WPAN to measure and collect information regarding interference. When such detailed information regarding interference is available, the schedule can be adjusted based on interference information to avoid it. The devices measure their signal and interference power levels over multiple fixed periods of time (superframes) and report back to the controller. The controller now has information to determine a schedule that avoids time slots reported to be subject to interference earlier. However, it must be noted that there is no interaction among the controllers of different networks, and each makes its scheduling decisions independent of the others. In the ideal case, if there are enough non-interfering slots to satisfy the time demands of previously interfering links, the respective controllers will eventually assign completely non-overlapping time slots to the links, and thus avoid interference fully.

Super-Controller — In this approach we assume there is coordination not only within each network but across all WPANs to measure and collect information regarding interference. This is equivalent to having a single *super-controller* that can coordinate among the controllers of individual WPANs. Although the details of how the super-controller coordinates among individual WPAN controllers is outside the scope of this work, we assume that the network architecture could be set up in such a way as to allow the super-controller to request link interference measurement information, and individual controllers to collect and report such information. Additionally, the super-controller is capable of scheduling *test transmissions* to figure out the link compatibility matrix; in other words, identifying the links that get interfered with by transmissions from particular links in neighboring networks. Making use of the network-wide link compatibility information, the super-controller can determine the schedule that causes the least interference.

Simulation Results

The scenario we consider is that of two 60 GHz links operating in adjacent cubicles in an enterprise environment, interfering with each other, as shown in Fig. 1 (Link1 and Link2). The 60 GHz link in each cubicle is assumed to carry compressed video from a laptop to a display. As for traffic generated, a burst of packets is generated every 250 μs, and the length of packets is drawn from Pareto distribution. The resulting stream has a mean data rate of 500 Mb/s and a maximum rate capped at 2.5 Gb/s. If there are no packet errors, an average sized video packet burst would take less than 50 μs to complete transmission, including acknowledgment (ACK) packets, at the highest data rate of 3.8 Gb/s. However, in order to accommodate larger bursts and packet errors, the station requests 115 μs of allocation every 250 μs time period.

Simulations are carried out using the OPNET simulation tool. PHY characteristics of 60 GHz links and a propagation model characterized as given previously is used. In the MAC layer a data packet transmission is immediately followed by an ACK packet and a retransmission of a lost packet up to two times. Video application packet loss is defined as when an application packet is not received at all (after original and two retransmissions), or is delayed by more than 30 ms based on the frame rate of 30 frames/s.

Figure 6a illustrates the MAC IM schemes

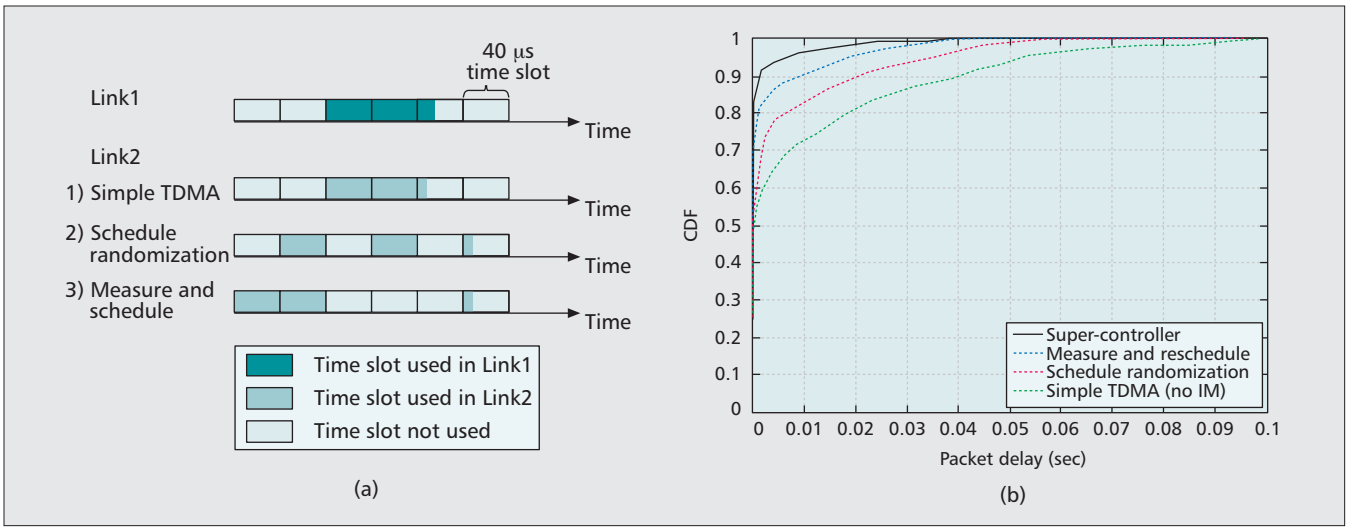

Figure 6. *Illustration of: a) different MAC IM schemes used in the simulations; b) video packet delay CDF comparison among MAC IM schemes.*

used in the simulations. In the schedule randomization technique, instead of allocating contiguous chunks of time, the scheduler divides time into discrete time slots (40 μs blocks), and allocates a total of 115 μs within 250 μs as three discrete time slots. The three slots are picked at random from the available six slots belonging to a given 250 μs period. For the measure and reschedule scheme, the fixed period of time (superframe) is divided into 10 μs time slots, and measurements are done for each such time slot. Finally, devices report back signal and/or interference power for every time block, averaged over multiple superframes. The controller, after collecting measurements from the devices, can determine the most appropriate slots to allocate for a particular stream. In our example the scheduler will select the three least interfering discrete time slots (40 μs × 3 = 120 μs) from the available six slots (240 μs). It is to be noted that the parameters chosen here can be optimized further to achieve better results, and is part of our ongoing research.

Figure 6b compares the CDF of video packet delay for the four MAC IM schemes described. The results correspond to a scenario shown in Fig. 6a, where for the simple TDMA scheme the schedules of the two links (Link1 and Link2) are fully overlapping with each other, and thus represent the worst case scenario. It is also noted here that any IM scheme is applied only when interference is detected, caused by partial or full overlap of time schedules. Qualitative results vary based on this assumption about initial overlap of schedules, but some general observations can be made as follows:

- Good IM mechanisms are needed, as indicated by the high amount of video loss without them. As an example, even for a less stringent delay budget of 30 ms, about 12 percent of packets fail to make it in time for the simple TDMA scheme.
- Better IM is possible as coordination and available information increases. Both the super-controller and measure and reschedule schemes achieve close to 0 percent packet drops for the 30 ms delay budget.
- It was observed that the measure and reschedule mechanism suffers from lack of convergence as the two networks measure and make scheduling decisions independently. When the measurement cycles were chosen to ensure convergence, results were significantly better.

Comparison

Figure 7 summarizes and compares the PHY and MAC IM techniques discussed in the previous sections in terms of performance and complexity. Complexity can be expressed in terms of the level of coordination required, amount of overhead messaging required, and implementation (hardware/software) complexity.

For the null-forming-based PHY IM technique, the direction of interference needs to be first estimated before performing null-forming. Although the null-forming technique performs well in most of the cases with a significant gain, if the directions of the interference source and the signal of interest are very close to each other (i.e., $\underline{\mathbf{s}}_0$ and $\underline{\mathbf{s}}_i$ have high correlation), the null-forming does not improve the link quality. In this case it may be better not to mitigate interference using the null-forming-based PHY IM scheme. As the number of antenna elements decreases, the beam width increases and thus it gets harder to mitigate interference close to the direction of the SOI. For example, a small form factor device may only have a small number of antenna elements, so the null-forming technique may not perform well. If the load of the network is low enough to move the time slots to non-interfering time slots relatively easily, instead of using the PHY IM technique, it may be better to enable one of the MAC IM techniques.

Regarding the MAC IM techniques we have studied here, a simple approach is to do schedule randomization. No specific information regarding the interferer is necessary. However, as with any randomized interference avoidance scheme, performance gains are limited. As the network load increases, the gains are especially

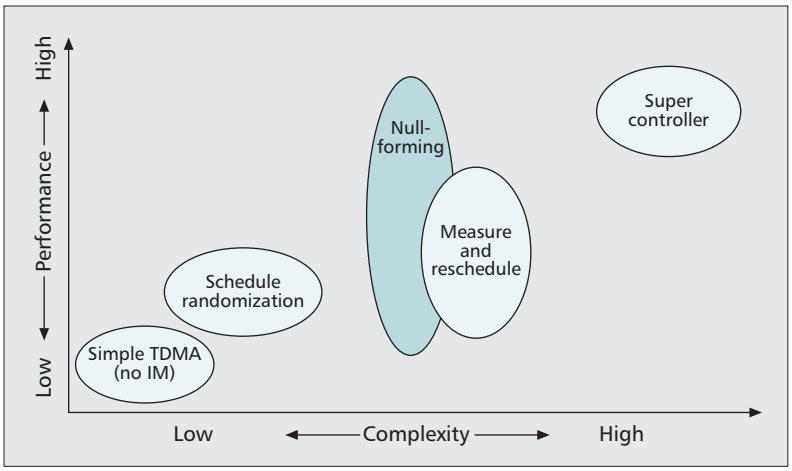

Figure 7. *Comparison of the interference mitigation (IM) schemes at PHY and MAC layers.*

low. Furthermore, the randomized schedule in a given network will make it even harder for a neighboring network to predict and avoid interference. In this sense, the scheme could contribute to more instability.

The measurement and rescheduling scheme depends on the ability to predict interference and alter scheduling to avoid interference. We have seen that when appropriate parameters are chosen, the scheme can perform well to mitigate interference. In particular, the issue of lack of convergence can degrade performance, although by careful selection of measurement periods, the new schedules can converge to non-interfering slots. Another practical aspect to consider is the overhead involved in reporting measurements and the power consumed to perform measurements. Finally, when interference does not lend itself to accurate prediction (when either the source or the schedule is random), IM gains are reduced. Overall, while measurement and rescheduling is promising, the gains are variable, and IM cannot be ensured in all cases.

The super-controller approach requires complete coordination among all the interfering WPANs, which associates with it the highest complexity. However, when such network architecture is available, the approach naturally works better than other MAC IM schemes in mitigating interference, and can ensure complete IM where it is possible.

Finally, it is noted that what we have presented here is not a comprehensive list of all possible techniques. As an example, using random access medium access protocol in place of TDMA could be an approach to mitigate interference and is the subject of our current study.

Conclusions

The unlicensed 60 GHz frequency band has great potential for wireless applications. However, due to the unlicensed nature of the band, wireless networks operating in the 60 GHz band are likely to suffer from interference. In order to guarantee the QoS of wireless video applications, the wireless devices operating in the unlicensed 60 GHz band will need PHY or MAC layer IM techniques, especially for a dense enterprise environment. This is clearly shown in the simulation results. Depending on the required performance and the complexity of coordination among the interfering networks, IM techniques should be carefully designed for wireless networks operating in the 60 GHz band.

Acknowledgments

The authors would like to thank the reviewers for excellent feedback. Helen K. Pan (Intel Labs) provided the antenna radiation pattern for the simulations and helped us understand various aspects of antenna designs in the 60 GHz band.

References

[1] S. K. Yong and C. Chong, "An Overview of Multigigabit Wireless through Millimeter Wave Technology: Potentials and Technical Challenges," *EURASIP J. Wireless Commun. Net.*, vol. 2007.

[2] J. M. Gilbert *et al.*, "A 4-Gbps Uncompressed Wireless HD A/V Transceiver Chipset," *IEEE Micro*, vol. 28, no. 2, 2008, pp. 56–64.

[3] ECMA TC48, "High Rate Short Range Wireless Communications"; http://www.ecma-international.org/memento/TC48-M.htm

[4] IEEE 802.15, "WPAN Millimeter Wave Alternative PHY Task Group 3c (TG3c)"; http://www.ieee802.org/15/pub/TG3c.html

[5] WirelessHD 1.0; http://www.wirelesshd.org/

[6] IEEE 802.11, "Very High Throughput in 60 GHz Task Group ad (TGad)"; http://www.ieee802.org/11/Reports/tgad_update.htm

[7] P. Smulders, "Exploiting the 60 GHz Band for Local Wireless Multimedia Access: Prospects and Future Directions," *IEEE Commun. Mag.*, vol. 2, no. 1, Jan. 2002, pp. 140–47.

[8] L. C. Godara, "Application of Antenna Arrays to Mobile Communications, Part II: Beam-Forming and Direction-of-Arrival Considerations," *Proc. IEEE*, vol. 85, no. 8, Aug. 1997, pp. 1195–1245.

[9] H. Xu, V. Kukshya, and T. Rappaport, "Spatial and Temporal Characteristics of 60 GHz Indoor Channels," *IEEE JSAC*, vol. 20, no. 3, Apr. 2002, pp. 620–30.

[10] M. Park and P. Gopalakrishnan, "Analysis on Spatial Reuse and Interference in 60-GHz Wireless Networks," *IEEE JSAC*, vol. 27, no. 8, Oct. 2009, pp. 1443–52.

Biographies

Minyoung Park (minyoung.park@intel.com) received his B.S. and M.S. degrees from Yonsei University, Seoul, Korea, in 1993 and 1995, respectively and his Ph.D. degree from the University of Texas at Austin in 2005, all in electrical engineering. From 1995 to 2001 he worked as a senior research engineer at LG Electronics Inc. Since 2005 he has been with Intel Labs as a research scientist. His research interest is in physical and MAC layers of wireless communications systems.

Praveen Gopalakrishnan obtained his M.S. degree in electrical engineering in 2003 specializing in wireless communications from WINLAB, Rutgers University, New Jersey. From 2003 to 2006 he worked as a research scientist at Telcordia Technologies, New Jersey, and since then at Intel Labs. He has been working on wireless MAC and system research issues, especially on WLAN and 60 GHz systems.

Richard Roberts [M] is an Intel Labs (Oregon) wireless research scientist working in the area of short wavelength, highly directional, layer one communications. This includes 60 GHz, Terahertz, and free space optics (FSO) such as visible light communications. He has a Ph.D. from Florida Institute of Technology.